

Quantum Control of Molecular Gas Hydrodynamics

S. Zahedpour, J. K. Wahlstrand, and H. M. Milchberg*

Institute for Research in Electronics and Applied Physics, University of Maryland, College Park, Maryland 20742, USA

(Received 24 October 2013; published 7 April 2014)

We demonstrate that strong impulsive gas heating or heating suppression at standard temperature and pressure can occur from coherent rotational excitation or deexcitation of molecular gases using a sequence of nonionizing laser pulses. For the case of excitation, subsequent collisional decoherence of the ensemble leads to gas heating significantly exceeding that from plasma absorption under the same laser focusing conditions. In both cases, the macroscopic hydrodynamics of the gas can be finely controlled with ~ 40 fs temporal sensitivity.

DOI: 10.1103/PhysRevLett.112.143601

PACS numbers: 42.50.Md, 42.50.Ct, 42.50.Wk

Significant hydrodynamic perturbation of solids, liquids, and nondilute gases by nonlinear absorption of intense laser pulses typically proceeds by localized plasma generation, which provides the pressure and temperature gradients to drive both mass motion and thermal transport. This is typically assumed to be the case for femtosecond filaments in gases, where depletion of the laser pulse energy due to absorption limits their ultimately achievable length [1] and where the thermal energy deposited in the gas can result in sound wave generation [2–9] followed by a gas density depression or “hole” that can persist on millisecond time scales [5–7]. Recently, it was shown that this density hole can affect filamentation at kilohertz repetition rates by acting as a negative lens [5] and can steer filaments [6]. It may even play an important role in filament-triggered electrical discharges [3,4]. New applications such as high average power laser beam guiding and remote generation of lensing structures in the atmosphere [7] can be enabled by control of energy deposition in gases by femtosecond laser pulses.

Previous work on energy deposition by filamentation has emphasized laser absorption due to atomic or molecular ionization and heating of free electrons [3–5,10]. In this Letter, we first show that molecular rotational heating is the dominant source of energy absorption in air filaments produced by single pulses. We then show that significantly greater gas heating can be generated by coherently and resonantly exciting a molecular rotational wave packet ensemble by a sequence of short nonionizing laser pulses separated by the rotational revival period [11,12]. By “wave packet,” we mean the coherent superposition of rotational eigenstates $|j, m\rangle$ excited by the laser pulse(s), where j and m are quantum numbers for rotational angular momentum and for the component of angular momentum along the laser polarization. Gas heating occurs by collisional deexcitation and decoherence of the ensemble, leading to a significant hydrodynamic response. Gas heating can be equivalent to that driven by a filament plasma heated up to ~ 50 eV, greatly in excess of typical filament plasma

electron temperatures of less than 5 eV. Moreover, we show that it is possible to deplete a population of rotationally excited molecules before the wave packet collisionally decoheres, suppressing gas heating. These results point to new ways of precisely controlling gas density profiles in atmospheric propagation [7], and have practical implications for schemes using pulse trains to enhance supercontinuum generation, filament length and plasma density [13,14], and THz amplification [11]. Other novel extensions are also suggested. Isotope-selective pumping of rotational population was measured recently at low temperatures and pressures [15]. The interferometric technique employed here, combined with optical centrifuge techniques [16,17] or chiral pulse trains [18], could find use in studying laser-induced gas vortices [19].

Here, laser excitation and deexcitation of the molecular ensemble is monitored by direct interferometric measurement of the gas density depression produced by subsequent heating of the gas. A short laser pulse is absorbed by exciting rotational population by a two-photon Raman process [20,21]. Gas heating occurs from thermalization of the pumped rotational ensemble, which occurs over hundreds of picoseconds [22]. Previously it was shown [5] that after $\sim 1 \mu\text{s}$, a pressure-balanced quasiequilibrium forms where the gas density profile is given by $\Delta N \approx -N_0 \Delta T / T_0$, where N_0 and T_0 are the background density and temperature and ΔT is the temperature increase from the laser absorption. Thus, the initial hole depth $|\Delta N|$ is proportional to the absorbed energy. The temperature profile, and therefore the density depression, then decays on millisecond timescales by thermal diffusion [5]. Even after many microseconds of diffusive spreading of the density hole [5], the peak depression is still proportional to the initial temperature, as verified in Fig. 1(a), in which a fluid code simulation [5] demonstrates the linear dependence of relative hole depth after $40 \mu\text{s}$ of evolution vs the initial gas temperature change in nitrogen.

A diagram of the experimental setup is shown in Fig. 1. The laser pump consisted of a single pulse, double pulse, or

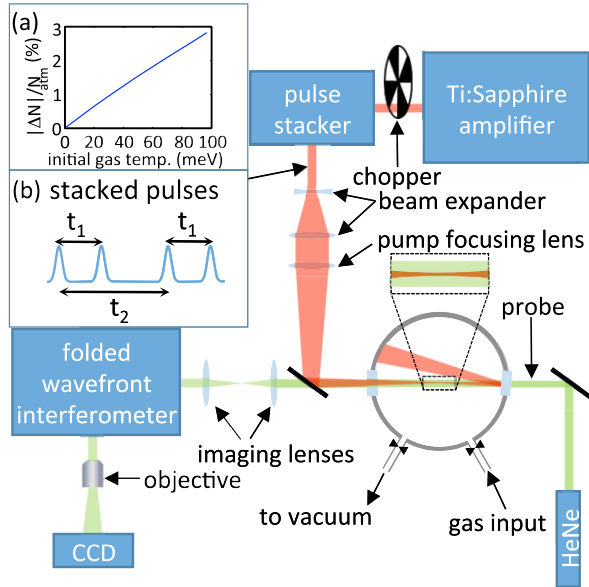


FIG. 1 (color online). Experimental setup for measuring the 2D density profile of the rotationally excited gas at the pump beam focus. The chopper provides alternating pump on and off for background subtraction. (a) Simulation of hole depth vs initial temperature showing that density hole depth is an excellent proportional measure of initial gas heating. (b) Scheme for (t_1, t_2) delay scan of pulses from the pulse stacker.

a train of four 800 nm, ~ 110 fs Ti:sapphire pump pulses generated with a 4-pulse Michelson interferometer [23] (“pulse stacker”). The beam was focused at $f/44$ by a lens into a chamber filled with various gases, to a vacuum beam waist FWHM of $33 \mu\text{m}$ and a confocal parameter of $2z_0 = 6.2$ mm. In all of the experiments, the laser was operated at 20 Hz to avoid the cumulative effects of long time scale density depressions caused by previous pulses [5]. A continuous wave helium-neon laser at $\lambda = 632.8$ nm provided a 2D interferometric probe of the gas density profile. A plane at the pump beam waist was imaged into a folded wave front interferometer and onto a CCD camera. Pump-induced changes in the gas density cause phase shifts $\Delta\varphi(x, y)$ in the z -propagating probes that are found by Fourier analysis of the interferogram [5]. Temporal gating of the probe pulse was achieved by triggering the CCD camera’s minimum $\sim 40 \mu\text{s}$ wide electronic shutter to include the pump pulse at the window’s leading edge. Before phase extraction, 50 interferograms were averaged in order to improve the signal-to-noise ratio [24]. This reduced the rms phase noise to ~ 6 mrad, enabling measurement of relative gas density changes $|\Delta N/N|$ as small as 10^{-4} . The probe interaction length in the pump-heated gas is the pump beam confocal parameter, $L \approx 2z_0$. The gas density depression profile is given by $\Delta N(x, y) = (\lambda/2\pi)\Delta\varphi(x, y)N_{\text{atm}}/[(n_{\text{atm}} - 1)L]$, where $N_{\text{atm}} \approx 2.47 \times 10^{19} \text{ cm}^{-3}$ is the molecular density at 1 atm and room temperature and n_{atm} is the index of refraction of the test gas at 1 atm [25].

In a preliminary experiment, we examined rotational absorption of single 110 fs pulses with energies ranging from 20 to 500 μJ ; Fig. 2 shows the peak relative density hole depth $|\Delta N_{\text{peak}}|/N_{\text{atm}}$ measured at the center of the profile, as a function of the vacuum peak intensity. Measurements are shown for 1 atm N_2 , O_2 , Ar, and air. As discussed above, $|\Delta N_{\text{peak}}|/N_{\text{atm}}$ is proportional to the laser energy absorption and initial gas temperature change. It is seen that its power dependence is quite different for the diatomic gases and Ar. For peak pump intensities of 40 TW/cm^2 , below the ionization threshold of argon, we measured induced density depressions in all the diatomic gases, but none in argon to within our measurement uncertainty. At intensities below their ionization thresholds, the energy absorbed by N_2 and O_2 has a roughly quadratic dependence on intensity, as expected for two-photon Raman absorption [8]. The curves deviate from the quadratic dependence at higher intensity, where absorption due to ionization strongly contributes. In all gases, saturation is observed at high pulse energy, which we attribute to the limiting of the laser intensity due to plasma defocusing [1]. Notably, our results show that at typical femtosecond filament clamping intensities of $\sim 50 \text{ TW}/\text{cm}^2$, the dominant source of laser energy deposition in molecular gases is rotational absorption and not ionization and plasma heating.

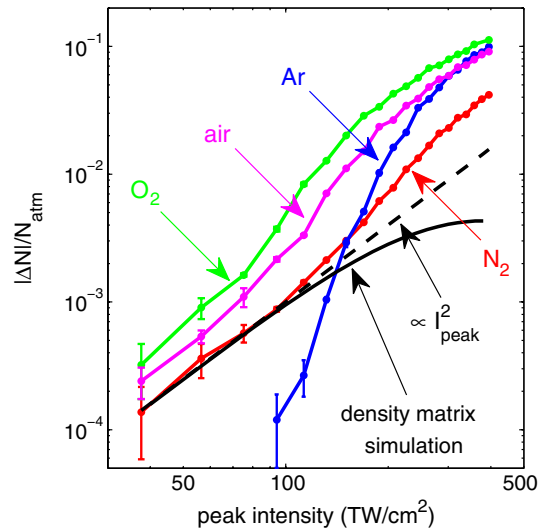


FIG. 2 (color online). Relative density depression (proportional to heating) measured at $40 \mu\text{s}$ delay due to single-pulse (110 fs FWHM) gas heating versus pump intensity at focus. In argon, plasma generation from multiphoton ionization and tunneling is the only source of gas heating, whereas in diatomic molecules, rotational excitation enables nonlinear absorption below the ionization threshold. The solid black line shows a density matrix calculation of the rotational absorption in N_2 and the dashed line is a classical calculation using Eq. (3). The experimental points deviate from the density matrix simulation at higher intensities due to ionization and plasma absorption, which is not modeled here.

To calculate rotational absorption, we numerically solve for the evolution of the density matrix ρ describing the ensemble of molecules [11,26,27],

$$\frac{d\rho}{dt} = -\frac{i}{\hbar}[H, \rho], \quad (1)$$

where $[\]$ denotes a commutator, and $H = H_0 + H_{\text{opt}}$ is the total Hamiltonian composed of $H_0 = \hat{L}^2/2I_M$ and the interaction between the optical field and the molecules, $H_{\text{opt}} = -\frac{1}{2}\mathbf{p} \cdot \mathbf{E}$. Here, \hat{L} is the rotational angular momentum operator, I_M is the moment of inertia of the molecule, \mathbf{p} is the induced dipole moment of the molecule, and \mathbf{E} is the laser pulse electric field. We note that for the parameters of our experiments, including the centrifugal term in H has negligible effect on the results. For copolarized optical pulses as used in our experiment, the interaction with the optical field only couples states with $\Delta j = \pm 2$ or 0 and $\Delta m = 0$. Initially at room temperature the rotational states are thermally populated, with the Boltzmann distribution peaking at approximately $j_{\text{max}} \sim 10$ in N_2 . The initial density matrix is $\rho_{jmjm'}^{(0)} = D_j \delta_{jj'} \delta_{mm'} \exp[-hcBj(j+1)/k_B T_0]/Z$, where k_B is Boltzmann's constant, $B = \hbar/(4\pi c I_M)$ is the rotational constant (2.0 cm^{-1} for N_2 [28]), $Z = \sum_k D_k (2k+1) \exp[-hcBk(k+1)/k_B T_0]$, and D_j is a statistical weighting factor depending on the nuclear spin. For N_2 , $D_j = 6$ for j even and $D_j = 3$ for j odd. The initial average rotational energy per molecule is $\text{Tr}(H_0 \rho^{(0)}) = k_B T_0$, where Tr is the trace operation. The change in average rotational energy ΔE per molecule (or the temperature change $k_B \Delta T$ of the molecular ensemble) induced by the pulse or pulse train is then given by

$$\begin{aligned} \Delta E &= k_B \Delta T = \text{Tr}[H_0 \rho(t_f)] - \text{Tr}(H_0 \rho^{(0)}) \\ &= \sum_{j,m} hcBj(j+1) \rho_{(j,m),(j,m)}(t_f) - k_B T_0, \end{aligned} \quad (2)$$

where $\rho(t)$ is evolved by Eq. (1) until time $t = t_f$ when the optical field from the pulse(s) is turned off. The pulse envelopes, individually or in a pulse train, are taken to be Gaussian in time.

The calculated rotational temperature change for a single pulse in N_2 is shown in Fig. 2 as a black solid line. The curve has been vertically shifted to match the experimentally measured hole depth in nitrogen. It matches well at low laser intensity I where rotational absorption is expected to be proportional to I^2 , but saturates at higher intensity as higher j states become more separated in energy. The low intensity dependence can also be modeled classically as follows. For a classical rigid rotor, the torque on a molecule due to an optical field polarized at an angle θ with respect to the molecular axis is $\frac{1}{2} \Delta\alpha |\mathbf{E}|^2 \sin 2\theta$ where $\Delta\alpha$ is the molecular polarizability anisotropy. The ensemble-averaged work done on a molecule in the limit of a single short pulse with fluence F is then

$$\Delta E_{\text{classical}} = \frac{16F^2 \pi^2 (\Delta\alpha)^2}{15c^2 I_M}. \quad (3)$$

This expression is plotted in Fig. 2 as a dashed line. The result agrees with the density matrix calculation at low intensities for a single pulse excitation of N_2 and O_2 . We emphasize that the density matrix calculation predicts only the rotational absorption—at high intensities, the absorption is dominated by ionization and plasma heating as seen in the increasing deviation of the experimental points and simulation curves.

In the next experiment we investigated the effect of a 4-pulse train on the laser absorption and heating in nitrogen. With multiple pulses timed to match the rotational revival period, it is possible to strongly enhance the contribution of higher rotational states to the wave packet ensemble [11]. Here we show directly that this translates into dramatically increased gas heating. The durations of pulses 1–4 were 110, 110, 120, and 110 fs, measured by a single shot autocorrelator, corresponding to vacuum peak intensities 61, 41, 41, and 51 TW/cm^2 . Note that if these pulses were coincident in time, the resulting single pulse would exceed the nitrogen ionization threshold. The pulse stacker time delays t_1 and t_2 were scanned by computer-controlled delay stages, so that the pulses arrived at $t = 0$, t_1 , t_2 , and $t_1 + t_2$, as depicted in Fig. 1(b). We initially tuned the time separation between successive pulses to be T , the period of the first rotational revival. In nitrogen, $T = (2cB)^{-1} \approx 8.36$ ps, the time when the alignment revival crosses zero. Then, a fine 2D scan in (t_1, t_2) of $|\Delta N_{\text{peak}}|/N_{\text{atm}}$ was performed with 40 fs steps.

Figure 3(a) shows the results of the pulse delay scan. Each point in the graph depicts the relative depth of the gas density hole at its center. The deepest hole, near $t_1 = T$ and $t_2 = 2T$, corresponds to the situation where each pulse in the train excites the molecules at the full revival from the previous pulse. Other features in the plot can be understood as resonances involving fewer pulses. The vertical bar ($t_1 = T$, $t_2 = 2T + \Delta t$) is where the first two pulses and second two pulses are resonant, but the delay between the second and third pulses is not. The horizontal bar ($t_1 = T + \Delta t$, $t_2 = 2T$) is where the first and third pulses are resonant (at the second full revival of the first pulse), and the same with the second and fourth pulses. The diagonals correspond to resonances between two pulses in the train. The southwest to northeast diagonal ($t_1 = T + \Delta t$, $t_2 = 2T + \Delta t$) is where the second and third pulses are resonant. The southeast to northwest diagonal ($t_1 = T + \Delta t$, $t_2 = 2T - \Delta t$) is where the first and fourth pulses are resonant (at the second half revival). The maximum depth of the gas density hole induced by the four-pulse train is ~ 6 times greater than the minimum in Fig. 3(a), which is similar to that induced by a single pulse.

Figure 3(b) shows a simulation, using Eqs. (1) and (2), of the absorbed energy in N_2 as a function of the (t_1, t_2) scan

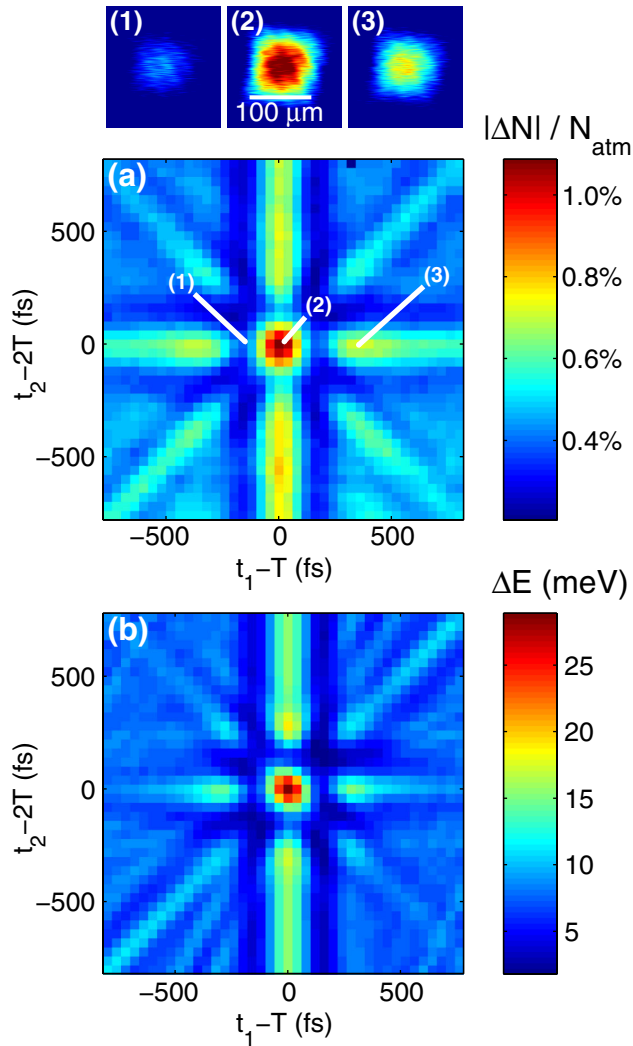


FIG. 3 (color online). Rotational absorption as a function of time delays t_1 and t_2 in the pulse stacker. The images at the top show extracted density hole images for three delays, showing the varying depth of the hole. (a) Interferometric measurement of peak relative depth of the gas density hole. The deepest gas density depression corresponds to the peak energy absorption predicted by the simulation. (b) Simulation of absorbed energy ΔE , found by numerically solving Eqs. (1) and (2) and averaging along the pump beam's confocal parameter.

of a four-pulse train using the experimental pulse parameters as inputs. The simulations predict ionization-free rotational heating of as much as ~ 32 meV/molecule ($\Delta T \sim 150$ K after thermal repartitioning) at the pump beam waist, which is only matched by a ~ 50 eV filament plasma (with electron density $\sim 10^{16}$ cm $^{-3}$ [29]). The plot shows an axial average peak heating of 28 meV/molecule along the pump confocal parameter. Comparison to Fig. 3(a) shows very good agreement between experiment and theory, with the resonance bars in the simulation decaying somewhat faster from the heating peak than in the experiment, an effect we are investigating. A similar

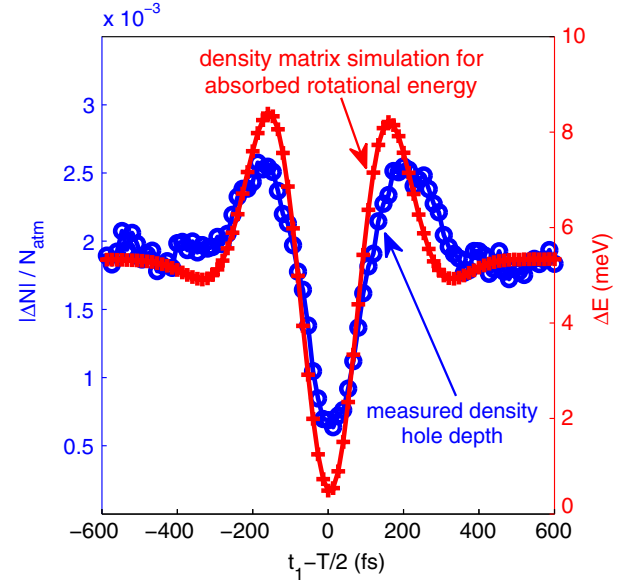


FIG. 4 (color online). Reduction of rotational heating using two pulses. Blue circles: Measured change in gas density as a function of the time delay t_1 between two pulses spaced near the half revival $T/2 \sim 4.18$ ps in N_2 . The hole depth is reduced by $\sim 65\%$. Red crosses: Simulation of rotational energy change per molecule from solving Eqs. (1) and (2) for varying t_1 , showing an absorption reduction of $\sim 90\%$.

experiment and simulation were performed for O_2 gas, likewise with good agreement.

So far we showed that it is possible to coherently excite a rotational wave packet ensemble with a sequence of pulses separated by a full revival period, leading to strong heating of a gas of diatomic molecules. However, it is also possible to first excite the ensemble and then deexcite it well within the decoherence time over which it would normally thermalize and fully heat the gas. To show this, we used the first two pulses out of the pulse stacker, as specified earlier. The first pulse was used to excite the ensemble. We scanned the arrival time of the second pulse, t_1 , near $T/2 \sim 4.18$ ps, the half-revival period of nitrogen. Figure 4 shows the measured depth of the density hole reduced by $\sim 65\%$ at the half-revival delay, while the simulation, axially averaged over the laser confocal parameter, shows an absorption reduction of $\sim 90\%$. In essence, energy from the first pulse invested in the wave packet ensemble is coherently restored to the second pulse. Viewed alternatively, the $T/2$ -delayed second pulse acts as an out-of-phase kick to suppress the molecular alignment induced by the first pulse, in contrast to the T -delayed pulses which act as in-phase kicks to enhance alignment.

In summary, we have measured the dramatic gas hydrodynamic response to coherent excitation and deexcitation of a molecular rotational wave packet ensemble, at peak laser intensities well below the ionization threshold. The laser absorption and gas heating is significantly enhanced

by using a four-pulse train with pulses separated by the molecular rotational revival time. Heating is strongly suppressed by coherently deexciting the molecular ensemble using pulses spaced by a half-revival. The femtosecond sensitivity to pulse train timing of gas heating and heating suppression is well predicted by density matrix simulations of the evolution of the wave packet ensemble. Our results make possible the fine quantum control of gas density profiles using nonionizing laser pulses. Such profile modification, at both near and remote locations, has a range of exciting applications including the refractive index control of high power optical pulse propagation in air [5–7].

The authors acknowledge useful discussions with J. Palastro. This work is supported by the Air Force Office of Scientific Research, the National Science Foundation, the Office of Naval Research, and the Department of Energy.

* milch@umd.edu

- [1] A. Couairon and A. Mysyrowicz, *Phys. Rep.* **441**, 47 (2007).
- [2] J. Yu, D. Mondelain, J. Kasparian, E. Salmon, S. Geffroy, C. Favre, V. Boutou, and J.-P. Wolf, *Appl. Opt.* **42**, 7117 (2003).
- [3] F. Vidal, D. Comtois, C.-Y. Chien, A. Desparois, B. La Fontaine, T. W. Johnston, J.-C. Kieffer, H. P. Mercure, H. Pépin, and F. A. Rizk, *IEEE Trans. Plasma Sci.* **28**, 418 (2000).
- [4] S. Tzortzakis, B. Prade, M. Franco, A. Mysyrowicz, S. Hüller, and P. Mora, *Phys. Rev. E* **64**, 057401 (2001).
- [5] Y.-H. Cheng, J. K. Wahlstrand, N. Jhajj, and H. M. Milchberg, *Opt. Express* **21**, 4740 (2013).
- [6] N. Jhajj, Y.-H. Cheng, J. K. Wahlstrand, and H. M. Milchberg, *Opt. Express* **21**, 28 980 (2013).
- [7] N. Jhajj, E. W. Rosenthal, R. Birnbaum, J. K. Wahlstrand, and H. M. Milchberg, *Phys. Rev. X* **4**, 011027 (2014).
- [8] D. V. Kartashov, A. V. Kirsanov, A. M. Kiselev, A. N. Stepanov, N. N. Bochkarev, Y. N. Ponomarev, and B. A. Tikhomirov, *Opt. Express* **14**, 7552 (2006).
- [9] A. M. Kiselev, Yu. N. Ponomarev, A. N. Stepanov, A. B. Tikhomirov, and B. A. Tikhomirov, *Quantum Electron.* **41**, 976 (2011).
- [10] Tz. B. Petrova, H. D. Ladouceur, and A. P. Baronavski, *Phys. Plasmas* **15**, 053501 (2008).
- [11] A. York and H. M. Milchberg, *Opt. Express* **16**, 10 557 (2008).
- [12] J. P. Cryan, P. H. Bucksbaum, and R. N. Coffee, *Phys. Rev. A* **80**, 063412 (2009).
- [13] S. Varma, Y.-H. Chen, J. P. Palastro, A. B. Fallahkhair, E. W. Rosenthal, T. Antonsen, and H. M. Milchberg, *Phys. Rev. A* **86**, 023850 (2012).
- [14] J. P. Palastro, T. M. Antonsen, Jr., and H. M. Milchberg, *Phys. Rev. A* **86**, 033834 (2012).
- [15] S. Zhdanovich, C. Bloomquist, J. Floß, I. Sh. Averbukh, J. W. Hepburn, and V. Milner, *Phys. Rev. Lett.* **109**, 043003 (2012).
- [16] D. M. Villeneuve, S. A. Aseyev, P. Dietrich, M. Spanner, M. Yu. Ivanov, and P. B. Corkum, *Phys. Rev. Lett.* **85**, 542 (2000).
- [17] L. Yuan, C. Toro, M. Bell, and A. S. Mullin, *Faraday Discuss.* **150**, 101 (2011).
- [18] S. Zhdanovich, A. A. Milner, C. Bloomquist, J. Floß, I. S. Averbukh, J. W. Hepburn, and V. Milner, *Phys. Rev. Lett.* **107**, 243004 (2011).
- [19] U. Steinitz, Y. Prior, and I. S. Averbukh, *Phys. Rev. Lett.* **109**, 033001 (2012).
- [20] H. Stapelfeldt and T. Seideman, *Rev. Mod. Phys.* **75**, 543 (2003).
- [21] C. H. Lin, J. P. Heritage, T. K. Gustafson, R. Y. Chiao, and J. P. McTague, *Phys. Rev. A* **13**, 813 (1976).
- [22] D. R. Miller and R. P. Andres, *J. Chem. Phys.* **46**, 3418 (1967).
- [23] C. W. Siders, J. L. W. Siders, A. J. Taylor, S. G. Park, and A. M. Weiner, *Appl. Opt.* **37**, 5302 (1998).
- [24] Y.-H. Chen, S. Varma, I. Alexeev, and H. M. Milchberg, *Opt. Express* **15**, 7458 (2007).
- [25] K. P. Birch, *J. Opt. Soc. Am. A* **8**, 647 (1991).
- [26] S. Ramakrishna and T. Seideman, *Phys. Rev. Lett.* **95**, 113001 (2005).
- [27] Y.-H. Chen, S. Varma, A. York, and H. M. Milchberg, *Opt. Express* **15**, 11 341 (2007).
- [28] K. P. Huber and G. Herzberg, *Molecular Spectra and Molecular Structure: IV. Constants of Diatomic Molecules* (Van Nostrand Reinhold, New York, 1979).
- [29] Y.-H. Chen, S. Varma, T. M. Antonsen, and H. M. Milchberg, *Phys. Rev. Lett.* **105**, 215005 (2010).